Power Flow Solution in Asymmetrical Multiconductor Systems

Roberto Benato, Antonio Paolucci†[1], Giovanni Gardan,
Department of Industrial Engineering, University of Padova, Padova

Received: 13 March 2021, Accepted: 3 April 2021, Published: 8 April 2021

***Abstract*—The power flow solution of a three-phase network can be more easily computed if the power system is assumed as having a symmetrical structure with balanced loads. In this way, only the single-phase positive sequence circuit can be considered since it is wholly representative of the balanced operation of the electrical system. However, technical literature has investigated general methods to compute power flow solution in asymmetrical/unbalanced situations, since these situations may occur in real networks, especially in the distribution ones. Thus, in this paper the authors provide an iterative algorithm (easily implementable into common PCs) for the study of asymmetrical-structure networks and with unbalanced load scenarios. This calculation approach is different from the classical numerical ones (e.g. Newton-Raphson and derived) and it is characterized by a high solution accuracy and low CPU time, even in ill-conditioned cases. Eventually, real case studies showing the existence of negative, zero sequence currents, and voltages in balanced-load and asymmetrical networks are presented.**

***Index Terms*—Asymmetrical Three-Phase Network, Multiconductor System, Three-Phase Power Flow, Unbalanced Loads.**

NOMENCLATURE

Symbol	Meaning
$\underline{\mathbf{Y}}$	complex admittance matrix
$\underline{\mathbf{Z}}$	complex impedance matrix
$\underline{\mathbf{v}}$	complex voltage vector
$\underline{\mathbf{i}}$	complex current vector
$\underline{v}$	complex voltage
$\bar{v}$	constrained voltage magnitude
$\underline{z}$	complex impedance
$\underline{y}$	complex admittance
$\underline{S}$	complex power
p	active power
q	reactive power
T	Fortescue matrix
R	incident matrix
U	identity matrix
Δ	elementary cell length of a line
n_c	number of elementary cells per line
d	line length
$\underline{\Delta\mathbf{i}}$	current injection vector
α	complex operator $= e^{j2\pi/3}$

Subscripts and superscripts

a	slack bus
x	generator buses b÷g
G	generator buses a÷g
L	load buses h÷ℓ
Sh	shunt elements
tr	transformer
f	phase component frame of reference
s	sequence component frame of reference
p	positive sequence
n	negative sequence
0	zero sequence *or* initial estimate (♣)
eq *or* equiv	equivalent
P	primitive (matrix)
1^{st}	first category element
2^{nd}	second category element
base	system base parameter
1,2, … k	first, second, …, k-th iteration
1,2,3	indices for: asynchronous user sets (1), static user sets (2), reactive power compensation devices (3)
*	complex conjugate
-1	matrix inversion
t	transposition

Abbreviations

HV	**H**igh-**V**oltage
EHV	**E**xtra **H**igh-**V**oltage
GIL	**G**as **I**nsulated transmission **L**ine
OHL	**O**ver**H**ead **L**ine
ACSR	**A**luminum **C**onductor **S**teel **R**einforced
p.u.	**p**er **u**nit

(♣) The symbol is used for more than one meaning, as it is specified.

I. INTRODUCTION

THIS paper is an updated translation of an Italian paper published in 2000 [1].

The power flow problem in a three-phase network is usually studied by means of the corresponding single-phase equivalent circuit.

However, the power quality in an electrical network can be studied more precisely if the considered three-phase system is thought as a multiconductor one, considering each phase coupled with other conductors (e.g. ground wires of overhead lines and metallic screens of insulated cables), and considering the unavoidable asymmetrical structure of the phase conductors.

Typical asymmetrical multiconductor components are the high and extra-high voltage overhead lines with one or more

[1] Died on 28/06/2014.

ground wires, because of the absence of symmetrical configuration of their phase conductors (often not transposed).

On the other hand, both single-core cable systems with a possible earth continuity conductor and long GILs (Gas Insulated transmission Lines) are asymmetrical systems.

In particular, the latter have been deeply investigated in the research field of electrical energy transmission since they are characterized by high performances and low electromagnetic and environmental impact.

Power flow solution in multiconductor systems can be a useful tool to check the presence of negative and zero sequence voltages and currents, even if generators, transformers and three-phase loads are considered structurally symmetric.

In this way, it is possible not only to assess the level of the electric power quality as seen at the final consumers, but also to check the presence of distortion in the system introduced by the network elements (especially by the generators) and involving measurement and protection devices. Moreover, power flow solution of such a system allows computing 50 Hz-magnetic fields in the proximity of the electrical lines, in order to make estimations on the environmental impact.

As shown in a subsequent paper, a multiconductor model can be a useful tool in order to study faulty regimes caused by simultaneous and multiple faults (asymmetrical short circuits and phase interruptions) in a simple and clear manner. In the technical literature, a lot of publications about power flow solutions have been presented [2-4], but the most established calculation methods are based on Newton-Raphson [5-9] and derived ones [10-13]. In particular, very interesting contributions deal with the modelling of the elements constituting the three-phase network [14].

In this paper, power flow solution is achieved by means of a unique complex admittance matrix including all network elements, generators (slack one excluded) and loads. Then, the solution is obtained through an iterative pattern involving matrix partitioning in complex form, without the need of real/imaginary decomposition. In this way, the procedure can be thought as a generalization of the algorithm presented in [15], which is valid only for symmetrical systems.

Moreover, the method presented in this paper is easily self-implementable on common PCs and is characterized by good convergence properties, even in ill-conditioned cases (very long lines, lines with high *r/x* ratio and near to the voltage collapse).

Finally, the CPU time of this procedure is always shorter or comparable with the ones of other calculation methods and the solutions are characterized by a very high accuracy.

II. Essentials of the Method

The method is based on the formal possibility to build steady-state models for generators and loads of the power system, by means of (3×3) admittance matrices (phase component admittance matrices).

Each of these matrices represent the complex power absorptions/injections whenever the corresponding elements are subjected to a three-phase set of voltages.

Thus, once it is excited by a three-phase slack voltage, the system exchanges power with the shunt elements, which model both generators and loads (loads absorb complex power, generators inject it).

This approach characterizes the originality of the proposed method.

The entire system is initially set (see Sect. 5.2) to have an initial solution near to the real steady-state one.

Subsequently, with an iterative approach, the sensitiveness of the system is analysed, and solution adjustments are opportunely executed at each iteration until convergence.

In order to study the steady-state solution of such a system, three-phase models of each network device must be considered. Eventually, mutual couplings among phases must be taken into consideration [16].

These power network models can be divided into two categories:

1st) **One-section elements**, which are connected by only one section into the network (e.g. generators, loads, reactive shunts and filters);
2nd) **Two-section elements**, which are the network devices connected between two sections.

Each three-phase network element, which belongs to the first category or to the second one, is characterized by an admittance matrix which relates the currents and the voltages of each phase: in this way, it is quite easy to build the nodal admittance matrix which models the entire network.

Fig. 1 shows the basic idea of the phase component modelling: for a generic 1st) category element connected to the *i-th* section, currents and voltages column vectors (3×1) are related through a phase component admittance matrix (3×3) $\underline{\mathbf{Y}}_{\mathbf{i}}^{\mathbf{1st}}$; whereas for a generic 2nd) category element connected between the *i-th* and *j-th* sections, current and voltage column vectors (3×1) are related through a phase component admittance matrix (6×6) $\underline{\mathbf{Y}}_{\mathbf{ij}}^{\mathbf{2nd}}$.

For example, Appendix A.2 shows that a three-phase overhead line including two ground wires is wholly described by using a (10×10) matrix.

However, this (10×10) matrix can be reduced to a (6×6) phase component admittance matrix $\underline{\mathbf{Y}}_{\mathbf{ij}}^{\mathbf{2nd}}$, which considers (to power flow purposes) even the effects due to the presence of the two earthed ground wires. The matrices $\underline{\mathbf{Y}}_{\mathbf{i}}^{\mathbf{1st}}$ and $\underline{\mathbf{Y}}_{\mathbf{ij}}^{\mathbf{2nd}}$ are not sparse, since they include the mutual admittances due to the phase couplings.

However, for the study of asymmetrical three-phase networks, it is necessary to make a phase component modelling not only for asymmetrical devices (OHL lines), but also for structurally symmetrical devices (e.g. power transformers and synchronous generators).

In order to study a three-phase electrical system, the considered network can be splitted into two blocks as shown in Fig. 2: the *passive network block **N** with all its n sections* $a \div \ell$, which includes the set of distribution and interconnection elements, and the *shunt element block **Sh***, which includes both loads **L** and generators **G**, excluding the slack generator (so $\underline{\mathbf{Y}}_{\mathbf{a}} \equiv \mathbf{0}$), since it must be considered as the external element exciting the whole system.

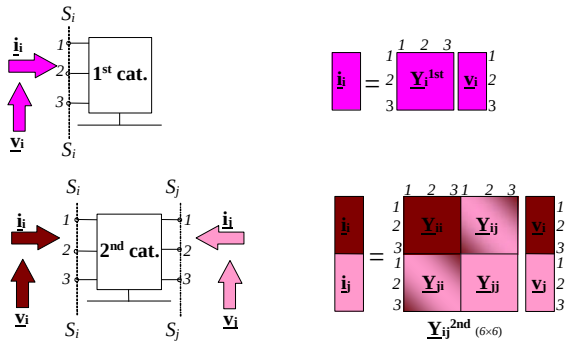

Fig. 1. Phase-modelling representation of the 1st) and the 2nd) category network elements.

The first block is represented by a ($3n\times3n$) phase component admittance matrix $\underline{\mathbf{Y}}_N$, whereas the second one is represented by a same-dimension admittance matrix $\underline{\mathbf{Y}}_{Sh}$. In the paper, all the elements of the abovementioned matrices are considered in p.u.

For the **N** block, according to voltage and current sign conventions shown in Fig. 2, the following equation can be written:

$$\underline{\mathbf{i}}_N = \underline{\mathbf{Y}}_N \underline{\mathbf{v}} \qquad (1)$$

where:

$$\underline{\mathbf{i}}_N = \left[\underline{\mathbf{i}}_{aN}^t \;\; \underline{\mathbf{i}}_{bN}^t \;\; .... \;\; \underline{\mathbf{i}}_{gN}^t \;\; \underline{\mathbf{i}}_{hN}^t \;\; .... \;\; .... \;\; .... \;\; \underline{\mathbf{i}}_{\ell N}^t\right]^t, \qquad (2)$$

$$\underline{\mathbf{v}} = \left[\underline{\mathbf{v}}_a^t \;\; \underline{\mathbf{v}}_b^t \;\; .... \;\; \underline{\mathbf{v}}_g^t \;\; \underline{\mathbf{v}}_h^t \;\; .... \;\; .... \;\; .... \;\; \underline{\mathbf{v}}_\ell^t\right]^t. \qquad (3)$$

Differently for the **Sh** block, the following equation can be written:

$$\underline{\mathbf{i}}_{Sh} = \underline{\mathbf{Y}}_{Sh} \underline{\mathbf{v}} \qquad (4)$$

where:

$$\underline{\mathbf{i}}_{Sh} = \left[\underline{\mathbf{0}} \;\; \underline{\mathbf{i}}_{bS}^t \;\; .... \;\; \underline{\mathbf{i}}_{gS}^t \;\; \underline{\mathbf{i}}_{hS}^t \;\; .... \;\; .... \;\; .... \;\; \underline{\mathbf{i}}_{\ell S}^t\right]^t$$

and $\underline{\mathbf{Y}}_{Sh}$ is the ($3n\times3n$) diagonal block matrix, in which every diagonal block element is a (3×3) matrix representing a generator or a load (see Fig. 3).

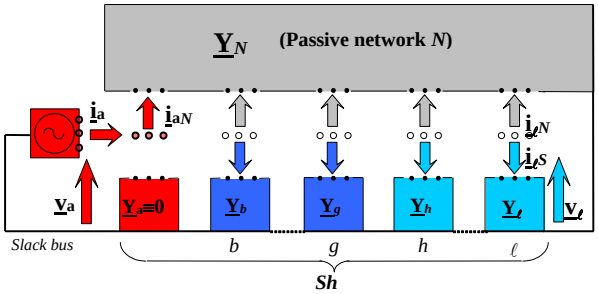

Fig. 2. Decomposition of a generic three-phase system into the passive network block ***N*** and the shunt block element ***Sh***.

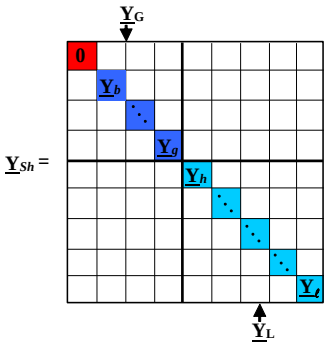

Fig. 3. Partitioned $\underline{\mathbf{Y}}_{Sh}$ matrix, holding the information about all network generators (except slack one) and loads.

Thus, once established $\underline{\mathbf{Y}}_N$ (see § 4.1) and $\underline{\mathbf{Y}}_{Sh}$, the steady-state solution of the system in Fig. 2 due to the application of $\underline{\mathbf{v}}_a$ must satisfy the following matrix equation:

$$\underline{\mathbf{i}} = \underline{\mathbf{Y}}\,\underline{\mathbf{v}} \qquad (5)$$

which derives from the side-by-side summation of (1) and (4). Thus, the matrix $\underline{\mathbf{Y}}$ is $\underline{\mathbf{Y}}_N+\underline{\mathbf{Y}}_{Sh}$ and $\underline{\mathbf{i}} = \left[\underline{\mathbf{i}}_a^t \;\; \mathbf{0} \;\; \mathbf{0} \;\; \mathbf{0} \;\; \mathbf{0} \;\; \mathbf{0} \;\; \mathbf{0} \;\; \mathbf{0} \;\; \mathbf{0}\right]^t$ is the column vector representing the net entering currents into the n sections $a\div\ell$ of the system.

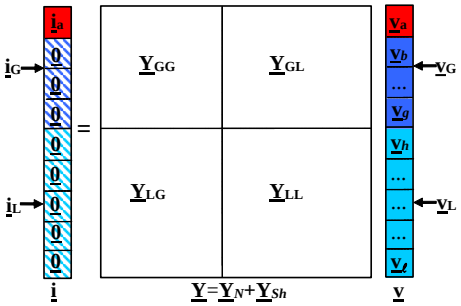

Fig. 4. Block partitioning of the matrix equation $\underline{\mathbf{i}}=\underline{\mathbf{Y}}\,\underline{\mathbf{v}}$.

By splitting $\underline{\mathbf{Y}}$, as shown in Fig. 4, it follows that:

$$\underline{\mathbf{i}}_G = \underline{\mathbf{Y}}_{GG}\,\underline{\mathbf{v}}_G + \underline{\mathbf{Y}}_{GL}\,\underline{\mathbf{v}}_L \qquad (6)$$

$$\underline{\mathbf{0}} = \underline{\mathbf{Y}}_{LG}\,\underline{\mathbf{v}}_G + \underline{\mathbf{Y}}_{LL}\,\underline{\mathbf{v}}_L. \qquad (7)$$

From (7), the expression of $\underline{\mathbf{v}}_L$ is:

$$\underline{\mathbf{v}}_L = -\underline{\mathbf{Y}}_{LL}^{-1}\underline{\mathbf{Y}}_{LG}\underline{\mathbf{v}}_G \qquad (8)$$

and its introduction in (6) yields:

$$\underline{\mathbf{i}}_G = \left[\underline{\mathbf{Y}}_{GG} - \underline{\mathbf{Y}}_{GL}\underline{\mathbf{Y}}_{LL}^{-1}\underline{\mathbf{Y}}_{LG}\right]\underline{\mathbf{v}}_G = \underline{\mathbf{Y}}_{Geq}\underline{\mathbf{v}}_G, \qquad (9)$$

where the matrix $\underline{\mathbf{Y}}_{LL}$ is generally nonsingular. Equation (9) can be represented as in Fig. 5.

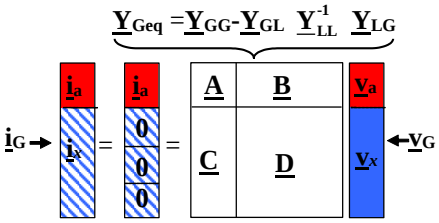

Fig. 5. Block partitioning of the matrix equation $\underline{\mathbf{i}}_G=\underline{\mathbf{Y}}_{Geq}\,\underline{\mathbf{v}}_G$.

It is worth noting that $\underline{\mathbf{Y}}_{Geq}$ characterizes the behaviour of the whole system as seen at the generator sections. In fact, $\underline{\mathbf{Y}}_{Geq}$ is the matrix that summarizes the interaction among network, generators, and loads. Once introduced the partitions shown in Fig. 5 and by observing that the subvector $\underline{\mathbf{i}}_x$ has all the components equal to zero, it results:

$$\mathbf{0}=\underline{\mathbf{C}}\,\underline{\mathbf{v}}_a+\underline{\mathbf{D}}\,\underline{\mathbf{v}}_x. \qquad (10)$$

So, the voltage generator vector $\underline{\mathbf{v}}_x$ (regarding the set of three-phase voltages in sections *b*.....*g*) is given by:

$$\underline{\mathbf{v}}_x= -\underline{\mathbf{D}}^{-1}\underline{\mathbf{C}}\,\underline{\mathbf{v}}_a, \qquad (11)$$

where the $\underline{\mathbf{D}}$ square-matrix is generally nonsingular. In this way, all the elements of the vector $\underline{\mathbf{v}}_G$ are known, so the elements of the vector $\underline{\mathbf{v}}_L$ can be found with (8), whereas vector $\underline{\mathbf{i}}_a$ can be found with the following:

$$\underline{\mathbf{i}}_a = \underline{\mathbf{A}}\underline{\mathbf{v}}_a + \underline{\mathbf{B}}\underline{\mathbf{v}}_x \qquad (12)$$

which likewise derives from the matrix partitioning shown in Fig. 5. Therefore, once established $\underline{\mathbf{Y}}_N$ (the matrix modelling the passive network) and $\underline{\mathbf{Y}}_{Sh}$ (the matrix modelling both the generators and loads) the "excitation" due to the (*3×1*) slack voltage vector $\underline{\mathbf{v}}_a$ define the steady-state solution of the whole system (represented in Fig. 2), in which loads and generators absorb and inject their own complex power respectively.

III. Phase Component Modelling of the Synchronous Generator

Since a cylindrical rotor synchronous machine can be considered a high-symmetry device, its steady-state regime can be easily studied by means of the sequence networks represented in Fig. 6. In particular, for the positive sequence (where the mechanical power conversion to the electrical power happens) which injects the complex power $\underline{S}_p = p_p + jq_p$, the following relations can be written:

$$\underline{S}_p = -\underline{v}_p \underline{i}^*_p; \quad \underline{i}_p = -\frac{\underline{S}^*_p}{\underline{v}^*_p} = \underline{y}_e \underline{v}_p; \quad \underline{y}_e = -\frac{p_p}{\underline{v}^2_p} + j\frac{q_p}{\underline{v}^2_p}. \qquad (13)$$

Once established the complex power $\underline{S}_p$ injected and the positive-sequence magnitude of the voltage $\overline{v}_p$ the model of the machine (as seen at its network terminals and represented in Fig. 6a)) is completely determined. This representation is also useful to model the salient pole rotor synchronous generator at the positive sequence (supposing it as a symmetrical structure).

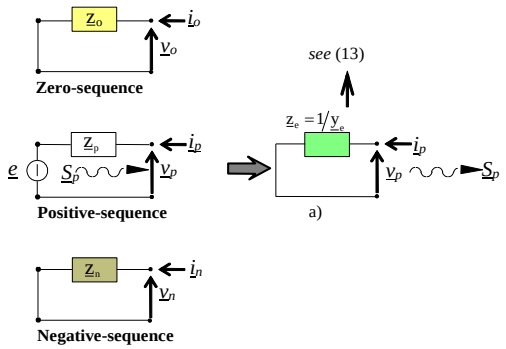

Fig. 6. Sequence component networks of the steady-state generators.

According to the method of the symmetrical components, the following sequence component diagonal matrix suitably represents the generator model:

$$\underline{\mathbf{Y}}_{gS} = \begin{bmatrix} \underline{y}_0 & & \\ & \underline{y}_e & \\ & & \underline{y}_n \end{bmatrix}$$

where $\underline{y}_o = 1/\underline{z}_o$; $\underline{y}_e = 1/\underline{z}_e$; $\underline{y}_n = 1/\underline{z}_n$. Since a generator is a symmetrical device, the knowledge of the phase values can be found by means of the Fortescue transformations (see Appendix A.1.). In this way, it is possible to find the (*3×3*) phase component admittance matrix $\underline{\mathbf{Y}}_g$:

$$\underline{\mathbf{Y}}_g=\mathbf{T}^{-1}\,\underline{\mathbf{Y}}_{gS}\,\mathbf{T} \qquad (14)$$

For the slack bus in § 5.1 a specific model is presented.

IV. $\underline{\mathbf{Y}}_N$ and $\underline{\mathbf{Y}}_{Sh}$ Construction

Once obtained the phase component matrices for each network component with the methods and the algorithms described in sections A.2. and A.3., the (*3n×3n*) $\underline{\mathbf{Y}}_N$ matrix must be built coherently with the topology of the network. Moreover, the (*3n×3n*) $\underline{\mathbf{Y}}_{Sh}$ block diagonal matrix must be built, and it describes the phase-behaviours of the generators and loads.

*4.1 The $\underline{\mathbf{Y}}_N$ building by means of $\underline{\mathbf{Y}}_P$ and **R** matrices*

Similarly to the single-phase study, in order to make automatic the construction of $\underline{\mathbf{Y}}_N$, it can be useful to use a primitive matrix $\underline{\mathbf{Y}}_P$ and an incident matrix **R**, which keeps the information about the topology of the network.

For the simple system represented in Fig. 7 (in which δ, ε, ζ represent three electrical lines) the diagram in Fig. 8 can be built (excluding the generators and the loads, according to Fig. 2). In this diagram the matrices **γ**, **δ**, **ε**, **ζ**, **η** characterize all the 2nd) category elements forming the network **N** and they are characterized by the currents $\underline{\mathbf{i}}^{\gamma}_a \div \underline{\mathbf{i}}^{\zeta}_{\ell}$ "injected" into their terminals.

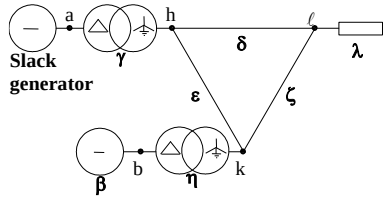

Fig. 7. Simple system with five sections and three derived elements.

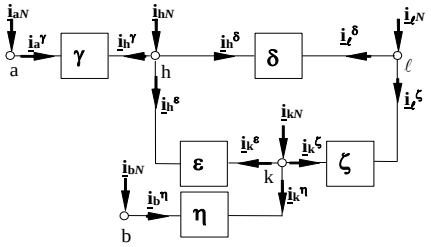

Fig. 8. Forming the matrices of the passive network N of Fig. 7.

Fig. 9 shows the matrix relation between voltage and current vectors of the two ends of each component. In this way, a unique matrix equation between nodal voltages and currents can be written:

$$\underline{\mathbf{i}}_P = \underline{\mathbf{Y}}_P \, \underline{\mathbf{v}}_P \qquad (15)$$

where the block-diagonal matrix $\underline{\mathbf{Y}}_P$ is called primitive matrix of the network.

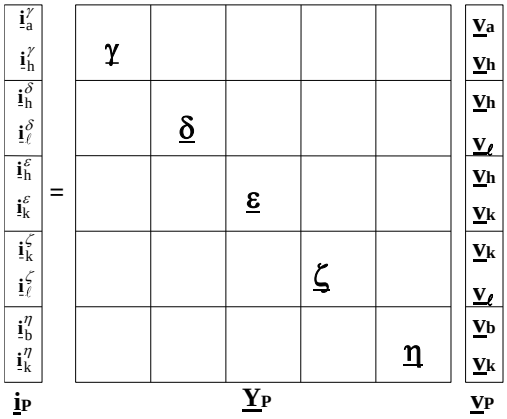

Fig. 9. Matrix structure of (15) for the Network of Fig. 7.

Fig. 10 shows that vector $\underline{\mathbf{v}}_P$ can be built by means of the incidence matrix $\mathbf{R}$ starting from the vector $\underline{\mathbf{v}}$ (which is composed of the voltages of sections $a \div \ell$). The matrix is built from the composition of $\mathbf{U}$, which are the *(3×3)* the identity matrices according to the following equation:

$$\underline{\mathbf{v}}_P = \mathbf{R} \, \underline{\mathbf{v}} \qquad (16)$$

It is worth noting in Fig. 11 that $\underline{\mathbf{i}}_N$ (whose components are the currents $\underline{\mathbf{i}}_{aN} \div \underline{\mathbf{i}}_{\ell N}$ entering the sections $a \div \ell$, according to Fig. 8) can be computed as

$$\underline{\mathbf{i}}_N = \mathbf{R}^t \, \underline{\mathbf{i}}_P \qquad (17)$$

where $\mathbf{R}^t$ is the transpose matrix of $\mathbf{R}$. By considering (15) and by combining (16) with (17), it follows:

$$\underline{\mathbf{i}}_N = \mathbf{R}^t \, \underline{\mathbf{Y}}_P \, \mathbf{R} \, \underline{\mathbf{v}} \qquad (18)$$

thus, $\underline{\mathbf{Y}}_N$ matrix of the network ***N*** of Fig. 8 (excluded generators and the load λ) is given by:

$$\underline{\mathbf{Y}}_N = \mathbf{R}^t \, \underline{\mathbf{Y}}_P \, \mathbf{R} \qquad (19)$$

Equation (19) is general and easily self-implementable, when the data of the networks are known.

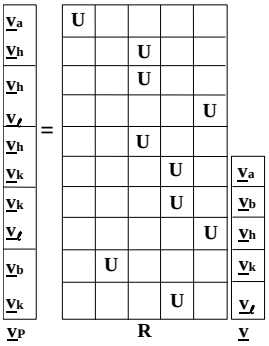

Fig. 10. Matrix from of (16) for the system represented in Fig. 7.

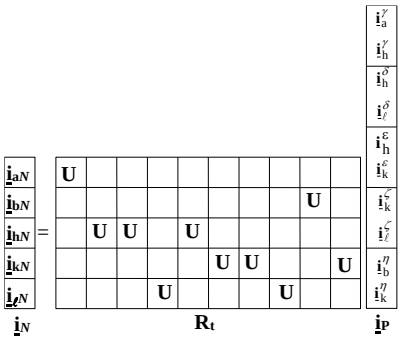

Fig. 11. Matrix from of (17) for the system represented in Fig. 7.

According to the present example, $\underline{\mathbf{Y}}_N$ is a block-sparse matrix, where the not-null submatrices are grey-highlighted in Fig. 12. Finally, by combining (15) and (16), it also follows that:

$$\underline{\mathbf{i}}_P = \underline{\mathbf{Y}}_P \, \mathbf{R} \, \underline{\mathbf{v}} \qquad (19b)$$

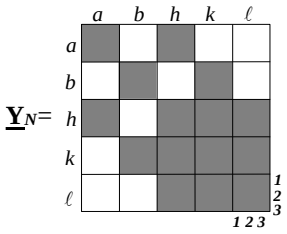

Fig. 12. Matrix $\underline{\mathbf{Y}}_N$ of the system in Fig. 7.

V. Power Flow Solution in Asymmetrical Systems

5.1 The asymmetrical system formulation

Firstly, it is convenient to precise that the constrained quantities necessary to calculate the power flow solution, for an asymmetrical system, are the following:

$\bar{V}_{pa}$	: positive-sequence voltage phasor of the slack-bus section *a*;
$\bar{v}_{pb} \ldots \bar{v}_{pg}$	: positive-sequence voltage magnitudes of the generator sections *b* ... *g*;
$\bar{p}_{pb} \ldots \bar{p}_{pg}$	: positive-sequence active power injected into the generator sections *b* ... *g*;
$\bar{p}_h + j\bar{q}_h \ldots \bar{p}_\ell + j\bar{q}_\ell$	: complex power (finite or null) *absorbed* by the load sections *h*...*ℓ* for the nominal positive sequence voltage magnitude.

(20)

Once established the constrained values (20) at the network buses, it is necessary to make the following specifications:

i) The slack bus generator (see Fig. 13) in section *a*, is supposed to be a finite-power generator; however, it must always guarantee the presence of a three-phase positive sequence voltage at its terminals. This positive sequence voltage is represented by means of the phasor $\bar{\mathrm{v}}_{pa}$, which is a reference having a zero angle. Since the network is characterized by some asymmetrical elements (e.g. overhead lines) and sometimes by unbalanced loads, it is predictable that the slack generator is characterized by the presence of both negative and zero sequence voltages and currents (whenever a possible downstream step-up transformer allows the circulation of zero-sequence currents).

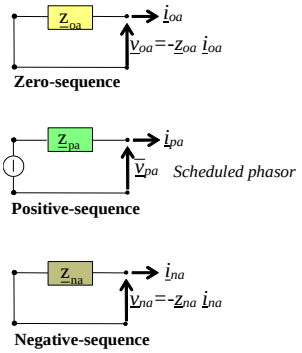

Fig. 13. Sequence component networks of the slack generator.

According to the symmetrical component networks of Fig. 13 (with the same current conventions of Fig. 2) the phase component elements of the vector $\mathbf{v_a}$ can be expressed by means of $\mathbf{T^{-1}}$ transformation (see Appendix A.1.):

$$\mathbf{v_a} = \begin{bmatrix} 1 & 1 & 1 \\ 1 & \alpha^2 & \alpha \\ 1 & \alpha & \alpha^2 \end{bmatrix} \cdot \begin{bmatrix} -Z_{oa}\dot{I}_{oa} \\ \bar{V}_{pa} \\ -Z_{na}\dot{I}_{na} \end{bmatrix} \qquad (21)$$

$\mathbf{T^{-1}}$ $\mathbf{v_{aS}}$

which is:

$$\mathbf{v_a} = \mathbf{T^{-1}} \begin{pmatrix} 0 \\ \bar{V}_{pa} \\ 0 \end{pmatrix} - \begin{bmatrix} Z_{oa} & & \\ & 0 & \\ & & Z_{na} \end{bmatrix} \mathbf{T} \begin{bmatrix} \dot{I}_{a1} \\ \dot{I}_{a2} \\ \dot{I}_{a3} \end{bmatrix} \qquad (22)$$

$\mathbf{i_a}$

where $\mathbf{T\, i_a = i_{aS}}$. Equation (22) is introduced in the adopted iterative pattern.

ii) For each iteration, the phase component vector $\mathbf{v_g}$ of a generic generator *g* can be decomposed into the components $\dot{V}_{og}, \dot{V}_{pg}, \dot{V}_{ng}$: the generator model (v. **iii**) must be adjusted until the magnitude of the positive sequence $\dot{V}_{pg}$ reaches the constrained value $\bar{V}_{pg}$.

iii) Since for the generator *g* the active power $\bar{P}_{pg}$ and the magnitude of the voltage $\bar{V}_{pg}$ are constrained, its solution adjustments consist of refreshing, according to (13), the imaginary part of $\dot{Y}_e$ (i.e. $Q_p / \bar{V}_p^{\,2}$), where Q_p is determined in each iteration according to the sensitiveness of the system, as it will be explained in the following.

iiii) Appendix A.4. shows that a three-phase load in parallel with a shunt for reactive power compensation can be correctly represented by the phase admittance matrix $\mathbf{Y_\ell}$ according to the participation of induction motors and static loads, once the complex power due to the application of a positive-sequence voltage is supposed. This fact corresponds to establish the block $\mathbf{Y_{LL}}$ as the nominal one regardless of the actual voltage in the loads. Moreover, the voltages are generally not so different from the nominal voltages. Anyway, the iterative adjustment of the phase admittance matrices is possible.

5.2. Initialization of the iterative procedure

It is useful to list the procedure steps as follows:

1) Building the matrix $\mathbf{Y_N}$ according to Sect. 4.1.

2) Building the sub-matrices $\mathbf{Y_h}$...$\mathbf{Y_\ell}$ related to loads, according to Appendix A.4., that remain constant during the entire procedure (nominal matrices).

3) Building the sub-matrices $\mathbf{Y_b^{(1)}} \ldots \mathbf{Y_g^{(1)}}$ related to the generators *b*÷*g* according to (13) and (14): as an example, for a generic generator *g*, $\dot{Y}_{eg}^{(1)}$ is calculated firstly, according to (13), with the following:

$$\dot{y}_{eg}^{(1)} = -\frac{\bar{P}_{pg}}{\bar{V}_{pg}^{\,2}} + j\frac{Q_{pg,0}}{\bar{V}_{pg}^{\,2}} \qquad (23)$$

where $\bar{P}_{pg}$ is the positive sequence active power (v. **iii**), $\bar{V}_{pg}$ is the constrained positive sequence magnitude and $Q_{pg,0}$ is the initial approximation of the reactive power generated in order to keep the voltage v_{pg} to the constrained level $\bar{V}_{pg}$. These initial approximations of $Q_{pg,0}$ can be easily computed according to the procedure shown in Fig.14. Supposing that generators (including the slack one) *a*÷*g* give the phase component vectors:

$$\mathbf{v_{a,0}} = \begin{bmatrix} 1 \\ \alpha^2 \\ \alpha \end{bmatrix} \bar{V}_{pa} \quad \ldots \quad \mathbf{v_{g,0}} = \begin{bmatrix} 1 \\ \alpha^2 \\ \alpha \end{bmatrix} \bar{V}_{pg} \qquad (24)$$

representing positive sequence sets, all in phase each other; the matrix $\mathbf{Y_{Sh,0}}$ is built by considering only the submatrices concerning loads and by setting the generators submatrices $\mathbf{Y_{a,0}} \equiv \mathbf{Y_{b,0}} \equiv \ldots \mathbf{Y_{g,0}} \equiv \mathbf{0}$.

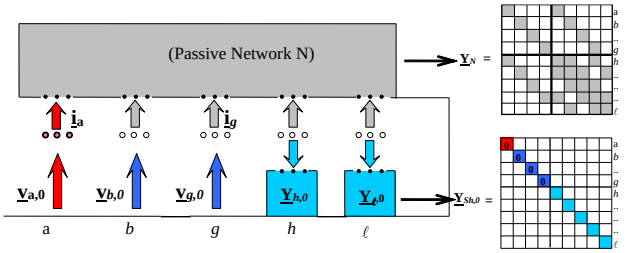

Fig. 14. Diagram representing the calculation of the initial reactive powers $\mathbf{q_{b,0}} \ldots \mathbf{q_{g,0}}$.

By splitting the following relation similarly to Fig. 4:

$$\underline{\mathbf{i}}=\underline{\mathbf{Y}}_0\,\underline{\mathbf{v}} \quad \text{where} \quad \underline{\mathbf{Y}}_0=\underline{\mathbf{Y}}_N+\underline{\mathbf{Y}}_{Sh,0} \tag{25}$$

and as for (6)÷(9), the following matrix relation can be obtained:

$$\underline{\mathbf{Y}}_{Geq,0}=\underline{\mathbf{Y}}_{GG,0}-\underline{\mathbf{Y}}_{GL}\,\underline{\mathbf{Y}}_{LL,0}^{-1}\,\underline{\mathbf{Y}}_{LG}$$

$$\begin{bmatrix}\underline{\mathbf{i}}_a\\ \underline{\mathbf{i}}_{x,0}\end{bmatrix}=\begin{bmatrix}\underline{\mathbf{A}}_0 & \underline{\mathbf{B}}_0\\ \underline{\mathbf{C}}_0 & \underline{\mathbf{D}}_0\end{bmatrix}\begin{bmatrix}\underline{\mathbf{v}}_{a,0}\\ \underline{\mathbf{v}}_{x,0}\end{bmatrix}\quad \underline{\mathbf{i}}_{G,0}\rightarrow \quad \leftarrow \underline{\mathbf{v}}_{G,0} \tag{26}$$

where the vector $\underline{\mathbf{i}}_{x,0}\neq\mathbf{0}$ representing the phase currents of the generators $b\div g$ result:

$$\underline{\mathbf{i}}_{x,0}=\underline{\mathbf{C}}_0\,\underline{\mathbf{v}}_{a,0}+\underline{\mathbf{D}}_0\,\underline{\mathbf{v}}_{x,0} \tag{27}$$

Thus, the Fortescue analysis of $\underline{\mathbf{v}}_{x,0}$ and $\underline{\mathbf{i}}_{x,0}$ allows computing the initial (approximated) reactive power for each generator $q_{dg,0}$ to be introduced in (23).

4) Building $\underline{\mathbf{Y}}^{(1)}=\underline{\mathbf{Y}}_N+\underline{\mathbf{Y}}_{Sh}^{(1)}$.

5) Partitioning $\underline{\mathbf{i}}^{(1)}=\underline{\mathbf{Y}}^{(1)}\underline{\mathbf{v}}^{(1)}$ according to Fig. 4.

6) Building $\underline{\mathbf{Y}}_{Geq}^{(1)}$ according to (9) and its partitioning according to Fig. 15; matrix $\underline{\mathbf{A}}_1$ (3×3); $\underline{\mathbf{B}}_1$ ($3\times3(n-1)$); $\underline{\mathbf{C}}_1$ ($3(n-1)\times3$); $\underline{\mathbf{D}}_1$ ($3(n-1)\times3(n-1)$) are obtained.

7) First iteration calculation of the phase vector $\underline{\mathbf{v}}_x^{(1)}$

$$\underline{\mathbf{v}}_x^{(1)}=-\underline{\mathbf{D}}_1^{-1}\underline{\mathbf{C}}_1\underline{\mathbf{v}}_a^{(1)} \tag{28}$$

in accordance with (11) and calculation of $\underline{\mathbf{v}}_a^{(1)}$ with (22), where $\underline{\mathbf{i}}_a\equiv\mathbf{0}$, due to the initialization.

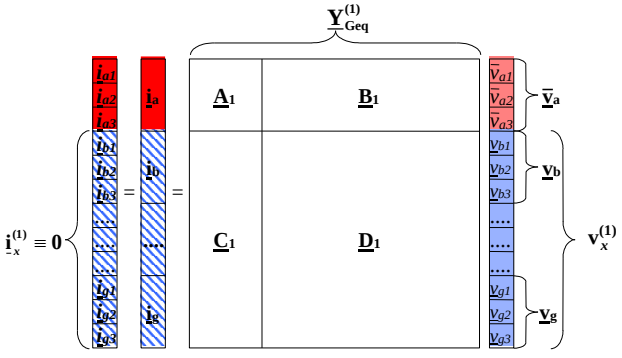

Fig.15. Matrix partitioning of the initial guess.

8) Calculating the first iteration sequence component voltage vector $\underline{\mathbf{v}}_{xS}^{(1)}$ of the generators $b\div g$ according to the following:

$$\begin{bmatrix}\underline{v}_{0b}^{(1)}\\ \underline{v}_{pb}^{(1)}\\ \underline{v}_{nb}^{(1)}\\ \dots\\ \dots\\ \dots\\ \underline{v}_{0g}^{(1)}\\ \underline{v}_{pg}^{(1)}\\ \underline{v}_{ng}^{(1)}\end{bmatrix}=\begin{bmatrix}\mathbf{T} & & \\ & \dots & \\ & & \mathbf{T}\end{bmatrix}\begin{bmatrix}\underline{v}_{1b}^{(1)}\\ \underline{v}_{1b}^{(1)}\\ \underline{v}_{3b}^{(1)}\\ \dots\\ \dots\\ \dots\\ \underline{v}_{1g}^{(1)}\\ \underline{v}_{2g}^{(1)}\\ \underline{v}_{3g}^{(1)}\end{bmatrix} \tag{29}$$

$\underline{\mathbf{v}}_{xS}^{(1)}$ $\quad \mathbf{T}_x$ $\quad \underline{\mathbf{v}}_x^{(1)}$

9) Calculating the first iteration phase current sub-vector $\underline{\mathbf{i}}_a^{(1)}$ of the slack bus:

$$\underline{\mathbf{i}}_a^{(1)}=\underline{\mathbf{A}}_1\underline{\mathbf{v}}_a^{(1)}+\underline{\mathbf{B}}_1\underline{\mathbf{v}}_x^{(1)} \tag{30}$$

5.3. The iterative pattern

The vector $\underline{\mathbf{v}}_{xS}^{(1)}$ obtained in the first iteration with (29) (which analyses the sequence components of the vector $\underline{\mathbf{v}}_x^{(1)}$) is characterized by the positive sequence components $\underline{v}_{pb}^{(1)}=v_{pb}^{(1)}\cdot e^{j\beta_1}\dots\underline{v}_{pg}^{(1)}=v_{pg}^{(1)}\cdot e^{j\gamma_1}$, whose magnitudes are generally different from the constrained ones:

$$v_{pb}^{(1)}\neq\bar{v}_{pb}\dots\dots v_{pg}^{(1)}\neq\bar{v}_{pg}\,.$$

By considering the correlation between reactive power and voltage magnitudes, reactive power q^* established as in **3)** must be iteratively adjusted by introducing reactive power injections $\Delta q_{pg}^{(1)}$ that change the admittances $\underline{y}_{eg}^{(2)}$ for each generator. In particular, the correction varies the value of the imaginary part:

$$\underline{y}_{eg}^{(1)}=-\frac{\bar{p}_{pg}}{\bar{v}_{pg}^2}+j\frac{q_{pg}+\Delta q_{pg}^{(1)}}{\bar{v}_{pg}^2} \tag{31}$$

Then, a new vector $\bar{\underline{\mathbf{v}}}_{xS}^{(1)}$ is considered, which is different from $\underline{\mathbf{v}}_{xS}^{(1)}$ (see Fig. 16), since the positive sequence voltage magnitudes are set to be equal to the constrained ones, the angles of $\bar{\underline{\mathbf{v}}}_{xS}^{(1)}$ are instead kept unchanged. The corresponding phase component corrected voltage vector is given by:

$$\bar{\underline{\mathbf{v}}}_x^{(1)}=\mathbf{T}_x^{-1}\cdot\bar{\underline{\mathbf{v}}}_{xS}^{(1)} \tag{32}$$

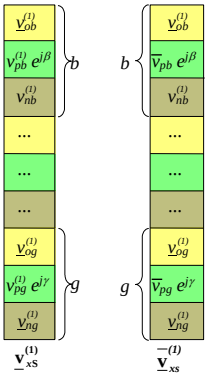

Fig. 16 Vectors $\underline{\mathbf{v}}_{xS}^{(1)}$ .and $\bar{\underline{\mathbf{v}}}_{xS}^{(1)}$

Equation (33) clearly highlights that the imposition of this vector is related to the injections of phase currents $\underline{\mathbf{\Delta i}}_{\mathbf{x}}^{(1)}$ (in the generator sections *b*÷*g*), which can be easily computed:

$$\underline{\mathbf{\Delta i}}_{\mathbf{x}}^{(1)} = \underline{\mathbf{C}}_1 \underline{\mathbf{v}}_{\mathbf{a}}^{(1)} + \underline{\mathbf{D}}_1 \underline{\mathbf{v}}_{\mathbf{x}}^{(1)} \tag{33}$$

The application of (34) links the phase component vector $\underline{\mathbf{\Delta i}}_{\mathbf{x}}^{(1)}$ with the sequence component vector $\underline{\mathbf{\Delta i}}_{\mathbf{xS}}^{(1)}$

$$\underline{\mathbf{\Delta i}}_{\mathbf{xS}}^{(1)} = \mathbf{T}_x \cdot \underline{\mathbf{\Delta i}}_{\mathbf{x}}^{(1)} . \tag{34}$$

The knowledge of $\underline{\mathbf{\Delta i}}_{\mathbf{xS}}^{(1)}$ allows extracting, for a generic generator *g*, the positive sequence $\underline{\Delta i}_{pg}^{(1)}$ injected into the section *g* in the steady-state regime resulting from the application of the constrained voltage. The injected current is linked to an injected positive-sequence complex power given by:

$$\Delta p_{pg}^{(1)} + j\Delta q_{pg}^{(1)} = \overline{v}_{pg}\, e^{j\gamma} \cdot \underline{\Delta i}_{pg}^{*(1)} \tag{35}$$

Since, for each generator, there is a close relationship between voltage magnitude and reactive power, it is quite reasonable to introduce in (31) the reactive correction $\Delta q_{pg}^{(1)}$ obtainable, for each generator, from (35) as shown in Fig. 17. Then, $\underline{y}_{eg}^{(2)}$ is used to obtain $\underline{\mathbf{Y}}_{\mathbf{G}}^{(2)}$ and its blocks $\underline{\mathbf{A}}_2$, $\underline{\mathbf{B}}_2$, $\underline{\mathbf{C}}_2$, $\underline{\mathbf{D}}_2$ used for the second iteration. It is worth noting that the rectangular matrixes $\underline{\mathbf{B}}_2$ and $\underline{\mathbf{C}}_2$ exactly correspond to $\underline{\mathbf{B}}_1$ and $\underline{\mathbf{C}}_1$. The corrections involving the positive sequence susceptances of the generators are connected to the "sensitiveness", expressed by (33) and by the corresponding ones of the next iterations of the passive network, as seen at buses *b*÷*g*.

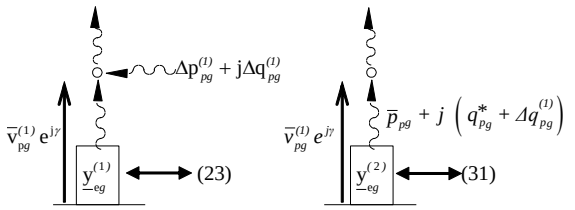

Fig. 17 Representation of $\underline{y}_{eg}$ (b÷g) adjournments.

Once obtained the convergence in the *k*-th iteration on the positive sequence voltage and active power constrained for the generator in (20), the steady-state regime of asymmetrical system can be completely computed, by considering "nominal models" for the loads, as specified in **iiii)**. The phase-vector $\underline{\mathbf{v}}_{\mathbf{L}}$, can be obtained by (8), i.e.

$$\underline{\mathbf{v}}_{\mathbf{L}}^{(\mathbf{k})} = -\underline{\mathbf{Y}}_{\mathbf{LL}}^{-1}\, \underline{\mathbf{Y}}_{\mathbf{LG}}\, \underline{\mathbf{v}}_{\mathbf{G}}^{(\mathbf{k})}$$

The vector $\underline{\mathbf{i}}_{\mathbf{L}}$ is given by (36), i.e.

$$\underline{\mathbf{i}}_{\mathbf{L}}^{(\mathbf{k})} = \underline{\mathbf{Y}}_{\mathbf{L}}\, \underline{\mathbf{v}}_{\mathbf{L}}^{(\mathbf{k})} \tag{36}$$

where $\underline{\mathbf{Y}}_{\mathbf{L}}$ is the block diagonal matrix of the "nominal loads".

Once obtained the power absorbed by the loads, the nominal load models could be in case adjourned to proceed with the subsequent iterations. The sequence analysis described in (A.1.1) allows knowing the asymmetry level of each system section. Regarding the analysis of GIL, please refer to [17-21].

VI. Examples of Asymmetrical Power Flow Calculations

The described algorithm is systematically tested for several case studies, aiming at analysing the negative and zero sequence presence. A first example deals with the distortion introduced by a typical *380 kV* overhead line (see Fig. 19) *300 km* long, which supplies a system of ℓ loads summarized by an equivalent matrix (see Fig. A.4.2.) placed at the receiving-end, whereas the sending-end is characterized by a pure positive sequence voltage. The load is conceived as a set composed of an asynchronous, a static and a compensation share, as explained in Appendix A.4. Table I reports the results by changing the share of the asynchronous part over the total load. As shown in Table I, the following observations can be drawn:

- The voltage asymmetry (i.e the ratio between negative-sequence and positive-sequence voltage) due to the presence of the structurally asymmetric line is equal to *3,12 %* (for a purely static load).
- The level of asymmetry of voltage and current is not equal for the purely static load, because of the asymmetry introduced by the 132 kV lines.
- By increasing the share of the asynchronous load, the voltage asymmetry decreases up to a percentage equal to a *1,66 %*, for the case of 60% of asynchronous share. The reason of this behaviour is due to the asymmetrical effect introduced by the high negative sequence admittance. This effect is combined with a high negative-sequence current absorption (reaching the percentage of *4,09 %* of the direct sequence current), which introduces losses in asynchronous loads and possible malfunctions at equipment and measurement instruments.

The magnitude of zero sequence voltage seems to be independent of the load composition and is always low (about *2 ‰*). Another case study is represented by the system in Fig. 18, which holds the characteristics of three generators, transformers, and loads. Each *380 kV* electrical line has got the typical Italian structure characterized by three bundled conductors (3 subconductors per phase) and two ground wires (see Fig. 19); the height of the phase from the ground is about *42 m*; and the two ground wires are ACSR with the diameter ϕ*=14,7 mm;* the average span length of the span is *300 m* and the earth resistance for the towers is *15 Ω*. The sections are 18 ($\mathbf{S_1}$÷$\mathbf{S_{18}}$) with *54* nodes. There are 7 sets of loads absorbing altogether a nominal complex power of *2352+j686* [*MW+jMvar*] (with a symmetrical voltage of *20 kV*). With a completely static load, the voltage asymmetry rate in section 9 is *1,78 %*. It is worth noting that this value is computed in the *380 kV* section, where the effect of the loads lessens, because of the *132 kV* sub-transmission lines and transformers.

TABLE I
PERCENTUAL EVALUATION OF THE ASYMMETRY AT THE RECEIVING-END ℓ

LOAD COMPOSITION	STATIC LOAD	30% ASYNCH. LOAD SHARE	60% ASYNCH. LOAD SHARE
$\underline{S}_{\ell}$=MW+jMvar	555,9+j99,5	556,4+j99,9	556,5+j100
$\lvert\underline{\mathbf{v}}_{\mathbf{n}}\rvert/\lvert\underline{\mathbf{v}}_{\mathbf{p}}\rvert$ **[%]**	3,12	2,01	1,66
$\lvert\underline{\mathbf{i}}_{\mathbf{n}}\rvert/\lvert\underline{\mathbf{i}}_{\mathbf{p}}\rvert$ **[%]**	2,99	3,48	4,09

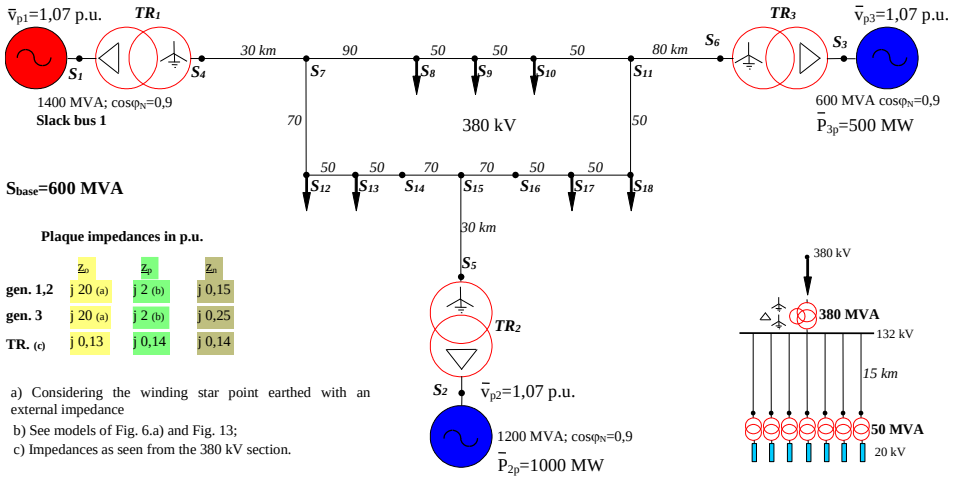

Fig. 18. Eighteen section system ($S_1 \div S_{18}$).

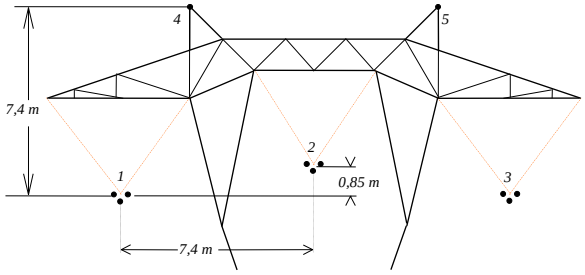

Fig. 19. Tower top of an overhead line 380 kV.

The actual asymmetrical rate on medium voltage (20 kV) is, by considering a load with an asynchronous component, less than the one computed in the 380 kV section, reducing to 0,8 %. Differently, in a completely static case, the asymmetry rate is quite the same comparing both the medium and the high voltage levels.

Another interesting aspect is represented by the negative-sequence currents injected by the synchronous generators; these currents together with the positive sequence ones define the real state of the electrical machines.

Table II summarizes the magnitudes of the three sequences for the generators, under the hypothesis of completely static loads.

Table III reports the case where all loads have got an asynchronous share equal to *60 %*. With completely static loads (Tab. II), the slack bus injects a negative sequence current equal to 4% of the positive current one, whereas for generators 2 and 3 these percentages are equal to *3,89 %* and *2,35 %*: the lesser percentage for the slack bus is due to the higher negative-sequence impedance (see parameters of Fig. 18). The zero-sequence currents injected by the generators are null, because the primary connection of the winding of the transformer is delta (dYN11).

TABLE II
MAGNITUDES OF THE SEQUENCE CURRENTS OF THE GENERATORS UNDER THE HYPOTHESIS OF PURE STATIC LOADS (NETWORK OF FIG. 18).

	SLACK BUS 1	GEN. 2	GEN. 3
$\lvert\underline{i}_0\rvert$ **[p.u.]**	0	0	0
$\lvert i_p\rvert$ **[p.u.]**	0,878	1,650	0,870
$\lvert i_n\rvert$ **[p.u.]**	0,035	0,064	0,021

TABLE III
MAGNITUDES OF THE SEQUENCE CURRENTS OF THE GENERATORS UNDER THE HYPOTHESIS OF A 60% ASYNCHRONOUS SHARE (NETWORK OF FIG. 18).

	SLACK BUS 1	GEN. 2	GEN. 3
$\lvert\underline{i}_0\rvert$ **[p.u.]**	0	0	0
$\lvert i_p\rvert$ **[p.u.]**	0,880	1,650	0,870
$\lvert i_n\rvert$ **[p.u.]**	0,010	0,060	0,010

The high asynchronous share (60% of the total load) involves a reduction of the asymmetry rate in the voltage in the load and generators sections, as shown in the first example. For instance, in section 9 the asymmetry rate ranges from *1,78 %* in the case of completely static load to *1,19 %* in the case of a load with a *60 %* of asynchronous motors, whereas the asymmetry rate goes from *1,65 %* to *2,88 %*. Table III shows how the current generators give a benefit because of the abovementioned considerations.

VII. CONCLUSIONS

The abovementioned procedure is implemented in MATLAB environment in a common PC. The procedure performances are characterized by satisfying CPU times, varying from 0,019 s to 0,12 s (with reference to the case study with 18 sections and 54 nodes and by adopting an Intel(R) Xeon(R) W-2125 CPU @ 4.00 GHz with 64 GB RAM) with positive sequence voltage mismatches varying from 10^{-4} to 10^{-14} p.u. Moreover, the procedure reaches high accuracy levels (converging even with a tolerance of 10^{-14} p.u.). Even if this level of accuracy is not necessary, this result is indicative of the robustness of the algorithm. All these results suggest that a matrix approach for the three-phase power flow solution can be a powerful tool without resorting to numerical analysis techniques as Newton-Raphson and derived.

APPENDIX I. THE FORTESCUE TRANSFORMATION

In this appendix, the Fortescue transformation [28] is briefly described. The phase component vectors (currents and voltages) $\underline{\mathbf{v}}_f$, $\underline{\mathbf{i}}_f$ and the corresponding sequence component vectors $\underline{\mathbf{v}}_s$, $\underline{\mathbf{i}}_s$ are represented as in the following:

$$\underline{\mathbf{v}}_f=\begin{bmatrix}\underline{v}_1\\ \underline{v}_2\\ \underline{v}_3\end{bmatrix};\ \underline{\mathbf{i}}_f=\begin{bmatrix}\underline{i}_1\\ \underline{i}_2\\ \underline{i}_3\end{bmatrix};\ \underline{\mathbf{v}}_S=\begin{bmatrix}\underline{v}_o\\ \underline{v}_p\\ \underline{v}_n\end{bmatrix};\ \underline{\mathbf{i}}_S=\begin{bmatrix}\underline{i}_o\\ \underline{i}_p\\ \underline{i}_n\end{bmatrix}.$$

It is well known that the Fortescue transformation allows passing from the symmetrical component frame of reference to the phase component one, so:

$$\underline{\mathbf{v}}_S=\underline{\mathbf{T}}\,\underline{\mathbf{v}}_f,\quad \underline{\mathbf{i}}_S=\underline{\mathbf{T}}\,\underline{\mathbf{i}}_f; \qquad (A.1.1)$$

$$\underline{\mathbf{v}}_f=\underline{\mathbf{T}}^{-1}\underline{\mathbf{v}}_S,\quad \underline{\mathbf{i}}_f=\underline{\mathbf{T}}^{-1}\,\underline{\mathbf{i}}_S; \qquad (A.1.2)$$

where the transformation matrices are:

$$\underline{\mathbf{T}}=\frac{1}{3}\begin{bmatrix}1 & 1 & 1\\ 1 & \alpha & \alpha^2\\ 1 & \alpha^2 & \alpha\end{bmatrix};\quad \underline{\mathbf{T}}^{-1}=\begin{bmatrix}1 & 1 & 1\\ 1 & \alpha^2 & \alpha\\ 1 & \alpha & \alpha^2\end{bmatrix};\quad \alpha=e^{j2\pi/3}$$

In particular, for a passive three-phase element with a symmetrical structure, the following relations can be written:

$$\begin{bmatrix}\underline{i}_o\\ \underline{i}_p\\ \underline{i}_n\end{bmatrix}=\begin{bmatrix}\underline{y}_o & & \\ & \underline{y}_p & \\ & & \underline{y}_n\end{bmatrix}\begin{bmatrix}\underline{v}_o\\ \underline{v}_p\\ \underline{v}_n\end{bmatrix}$$

$\underline{\mathbf{i}}_S$ $\underline{\mathbf{Y}}_S$ $\underline{\mathbf{v}}_S$

$\underline{\mathbf{i}}_S=\underline{\mathbf{Y}}_S\underline{\mathbf{v}}_S$; $\underline{\mathbf{T}}^{-1}\underline{\mathbf{i}}_S=\underline{\mathbf{T}}^{-1}\,\underline{\mathbf{Y}}_S\underline{\mathbf{v}}_S$; $\underline{\mathbf{i}}_f=(\underline{\mathbf{T}}^{-1}\,\underline{\mathbf{Y}}_S\,\underline{\mathbf{T}})\,\underline{\mathbf{v}}_f$ from which the phase component matrix $\underline{\mathbf{Y}}_f=\underline{\mathbf{T}}^{-1}\,\underline{\mathbf{Y}}_S\,\underline{\mathbf{T}}$ is deduced. Furthermore, for the complex power in p.u. $\underline{s}=\underline{S}_{three-phase}/S_{base}$, the following relationships in the two different frames of reference can be used:

$$\underline{s}=\underline{\mathbf{v}}_s^t\,\underline{\mathbf{i}}_s^*\quad\mapsto\quad \underline{s}=\underline{\mathbf{v}}_f^t\,\underline{\mathbf{i}}_f^*\cdot\frac{1}{3}.$$

Appendix II. The Phase Component Model of the Three-Phase Overhead Lines

The phase component model of a three-phase overhead lines is based on the general methodology used and verified by the authors in [22, 23] and well exposed in [24]. In order to model the entire line, the conductive wires (the phase conductors and the ground wires) are considered parallel among them and the earth and are considered as a cascade of n_c elementary cells of equal length Δ. Thus, by considering the classical theory of J.R. Carson [25, 26], the elementary cell matrix can be computed. Subsequently, from the essential procedure exposed in [17], the computation of the (*10×10*) matrix $\underline{\mathbf{Y}}_{\ell in}$ equivalent to the cascade composition of the n_c total cells can be made (the entire line length is $d=n_c\Delta$). Obviously, the dimension of $\underline{\mathbf{Y}}_{\ell in}$ is reduced to (*8×8)* when a unique ground wire is considered, whereas is reduced to (*6×6)* without the presence of any ground wire. However, it is quite logical that considering models of the dimension larger than (*6×6)* for the composition and the study of the entire electrical system implies onerous calculation procedures, because of the topological analysis and the calculation phase. In this section, the construction of power flow synthetic model considering only the three-phase conductors, but without neglecting the presence of the two ground wires, is shown. By means of the comparisons of different calculation results, it can be noted that even under the hypothesis of unearthed ground wires (see Fig. A.2.1.) ($i_{p5}=i_{p4}=i_{a5}=i_{a4}=0$), the effects on the phases, along the length of the line, are quite the same than the ones produced by the earthed ground wires. If the matrix $\underline{\mathbf{Y}}_{\ell in}$ is inverted, the obtained relation of Fig. A.2.1, where the currents injected in the ground wires are null, the behaviour of the phases (included the effects due to the ground wires) is summarised by the (*6×6*) matrix $\underline{\mathbf{Z}}_{\ell eq}$ obtained by means of the procedure of Fig. A.2.2.: the corresponding admittance matrix $\underline{\mathbf{Y}}_{\ell eq}$ summarizing the effects of the ground wires on the three phases is obtainable by the inverse of $\underline{\mathbf{Z}}_{\ell eq}$.

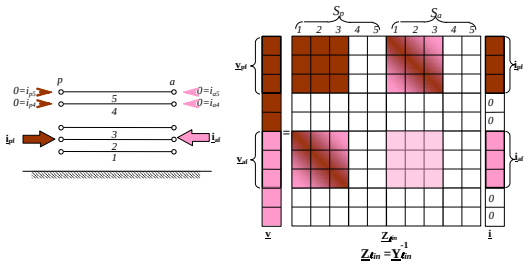

Fig. A.2.1. Matrix inclusion of the two ground wires of an overhead line.

$$\underline{\mathbf{Z}}_{\ell eq}=\begin{bmatrix}\cdot & \cdot & \cdot & \cdot & \cdot & \cdot\\ \cdot & \cdot & \cdot & \cdot & \cdot & \cdot\\ \cdot & \cdot & \cdot & \cdot & \cdot & \cdot\\ \cdot & \cdot & \cdot & \cdot & \cdot & \cdot\\ \cdot & \cdot & \cdot & \cdot & \cdot & \cdot\\ \cdot & \cdot & \cdot & \cdot & \cdot & \cdot\end{bmatrix};\quad \underline{\mathbf{Y}}_{\ell eq}=\underline{\mathbf{Z}}_{\ell eq}^{-1}\ \textbf{(6×6)}$$

Fig. A.2.2. Building the phase component admittance matrix $\underline{\mathbf{Y}}_{\ell eq}$.

The abovementioned criteria are still valid for other typologies (e.g. cables with metallic screens and longitudinal earth conductors [27]).

Appendix III. The Phase Component Model of the Three-Phase Transformer

In general, three-phase transformers are characterized by high-symmetry constructions: their typical sequence parameters (as short circuit impedances or the correspondence admittances in p.u.) allow formulating the phase component matrix $\underline{\mathbf{Y}}_{tr}$ by means of the Fortescue transformations.

A description of the procedure is shown in [24]; however, in this appendix, it is meaningful to mention a type of three-phase transformer (see A.3.1.) where the third winding is delta connected with the purpose of improving the zero sequence behaviour.

The zero-sequence treatment of the three-winding transformer produce a *T* circuit of three impedances (which can be obtained by the measurements between coupled windings) and therefore to a matrix $\underline{\mathbf{Y}}_0$ between *A* and *a*.

The composition of the sequence matrix and Fortescue transformations bring also in this case to a phase component matrix $\underline{\mathbf{Y}}_{tr}$. The presence of the earthed resistance of the substation, that could be easily implemented, can be neglected in the zero-sequence models, since it is characterized by low values and since the zero currents are very low when power flow studies of HV and EHV networks are considered.

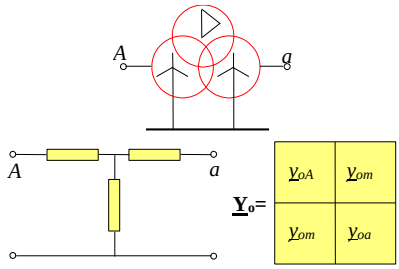

Fig. A.3.1. The matrix $\underline{Y}_o$ of the three-winding transformer.

Appendix IV. The Phase Component Modelling Of The Electrical Loads

The load ℓ can be conceived as being balanced and composed of:

1) a set of users, composed of asynchronous motors (loaded at their nominal power) absorbing a complex power equal to p_1+jq_1 in correspondence of the nominal positive sequence voltage;

2) a set of static loads absorbing p_2+jq_2, in correspondence of the nominal positive sequence voltage;

3) a reactive power compensation by means of a capacitor bank, absorbing a negative reactive power $q_3 = q_c$, in correspondence of the nominal positive sequence voltage.

Thus, the positive sequence nominal admittances (under a voltage of *1 p.u.*) can be easily computed by means of the systematic use of the following:

$$\underline{y} = \frac{p - jq}{1^2} \; [p.u.].$$

For each set of loads, excluding the absorption of the zero-sequence current, the admittance matrices are the following:

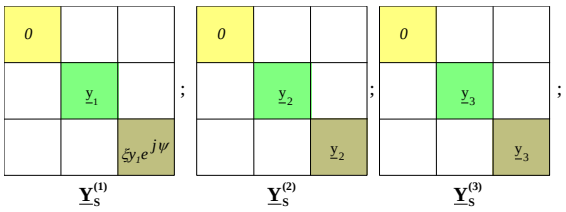

where for the static loads the positive and negative admittances are exactly the same; and for the set of asynchronous motors the negative sequence admittance (slip ~ *2*) is set equal to $\xi y_1 e^{j\psi}$, in which typically $\xi = 5 \div 7$ and $\psi = -60° \div -75°$.

The phase component matrix $\underline{\mathbf{Y}}_\ell$ characterizing the entire balanced load ℓ is therefore:

$$\underline{\mathbf{Y}}_\ell = \mathbf{T}^{-1} \left(\underline{\mathbf{Y}}_S^{(1)} + \underline{\mathbf{Y}}_S^{(2)} + \underline{\mathbf{Y}}_S^{(3)} \right) \mathbf{T} \, .$$

Moreover, the introduction of an additional set of unbalanced loads would involve, as shown in Fig. A.4.1., the phase component matrix $\underline{\mathbf{Y}}_{\ell sq}$ that can be built and summed to the matrix $\underline{\mathbf{Y}}_\ell$.

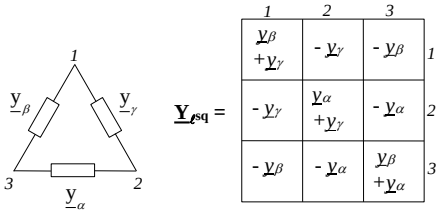

Fig. A.4.1. Modelling of an unbalanced load.

Finally, in many cases (see Fig. 18) an equivalent load scheme to the *380 kV* section ℓ can be usefully built, since the entire network as seen at section ℓ can be described by means of an equivalent matrix $\underline{\mathbf{Y}}_{equiv}$ (see Fig.A.4.2.).

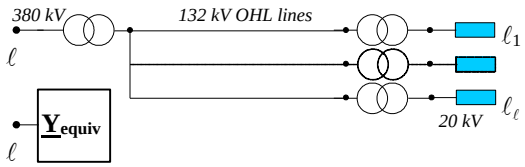

Fig. A.4.2. Equivalent matrix of the distribution network.

References

[1] R. Benato, A. Paolucci, "Power flow in multiconductor unbalanced systems. A PC-program", *L'Energia Elettrica*, 2000, 77, pp. 43–53 (in Italian).

[2] I. Dzafic and H. Neisius, "Generic Three-Phase Power Flow methods using symmetrical components for symmetrical and unsymmetrical power system networks,"*ISGT 2011*, Anaheim, CA, USA, 2011, pp. 1-6.

[3] D. M. Anderson and B. F. Wollenberg, "Solving for three phase conductively isolated busbar voltages using phase component analysis," in *IEEE Transactions on Power Systems*, vol. 10, no. 1, pp. 98-108, Feb. 1995.

[4] A. Tbaileh, B. A. Bhatti, R. Broadwater, M. Dilek and C. Beattie, "Robust Matrix Free Power Flow Algorithm for Solving T&D Systems," 2019 IEEE Power & Energy Society General Meeting (PESGM), Atlanta, GA, USA, 2019, pp. 1-5.

[5] R.G. Wasley, M.A. Shlash, "Newton-Raphson algorithm for 3-phase load flow". Proc. IEE, Vol. 121, N° 7, July 1974, pp. 630-638.

[6] X.-P. Zhang, H. Chen, "Sequence-Decoupled Newton-Raphson Three Phase Load Flow", presented at the *IEEE Region 10 International Conference TENCON*, Vol. 5, Beijing, China, 19-21 Oct. 1993.

[7] H. Le Nguyen, "Newton-Raphson Method in Complex Form", IEEE Trans. Power Syst., Vol, 12, No. 3, Aug. 1997, pp. 1355- 1359.

[8] P. A. N. Garcia, J. L. R. Pereira, S. Carneiro, M. d C. Vander, N. Martins, "Three-Phase Power Flow Calculations Using the Current Injection Method", IEEE Trans. Power Syst., Vol. 15, No. 2, May 2000, pp. 508- 514.

[9] X.-P. Zhang, P. Ju, E. Handschin, "Continuation Three-Phase Power Flow: A Tool for Voltage Stability Analysis of Unbalanced Three-

Phase Power Systems", IEEE Trans. Power Syst., Vol. 20, NO. 3, Aug. 2005, pp. 1320 – 1329.

[10] J. Arrillaga, B.J. Harker, "Fast-decoupled three-phase load flow." Proc. IEE, Vol. 125, N° 8, Aug. 1978, pp. 734-740.

[11] X.-P. Zhang, "Fast Three Phase Load Flow Methods", IEEE Trans. Power Syst., Vol. 11, No. 3, Aug. 1996, pp. 1547-1554.

[12] P.R. Bijwe, G. K. Viswanadha Raju, B. Abhijith, "Robust Three Phase Fast Decoupled Power Flow", presented at the *IEEE PES Power Systems Conference and Exposition, PSCE*, Seattle, WA, USA 15-18 March 2009.

[13] M. Abdel-Akler, K.M. Nor, A.H.A. Rashid, "Improved three-phase power-flow methods using sequence components", IEEE Trans. Power Syst., 01 Aug. 2005, pp. 1389– 1397.

[14] Mo-Shing Chen, William E. Dillon: Power System Modeling. *Proc.of the IEEE*, vol. 62, N° 7, July 1974, pp. 901-915.

[15] R. Benato, A. Paolucci, R. Turri, "Power Flow Solution by a Complex Admittance Matrix Method," *ETEP*, Vol. 10, N° 2, March-April 2001.

[16] R. Benato, *Advanced matrix techniques for the static and dynamic power systems analysis*. PhD thesis, Padova 1999 (in Italian).

[17] R. Benato, L. Fellin, D. Marzenta, A. Paolucci, "Gas-Insulated Transmission Lines: excellent performance and low environmental impact," *International Symposium and Exhibition on Electric Power Engineering at the Beginning of Third Millennium.* Napoli-Capri, 12-18 May 2000, pp. 385-405.

[18] R. Benato, F. Dughiero, M. Forzan, A. Paolucci, "Proximity Effect and Magnetic Field Calculation in GIL and in Isolated Phase Bus Ducts", *IEEE Trans. on Magnetics*, Vol. 38, No 2, marzo 2002, pp. 781– 784.

[19] R. Benato, F. Dughiero, "Solution of Coupled Electromagnetic and Thermal Problems in Gas Insulated Transmission Lines", *IEEE Trans. on Magnetics*, Vol. 39, No 3, May 2003, pp. 1741–1744.

[20] R. Benato, C. Di Mario, H. Koch, "High capability applications of Long Gas Insulated Lines in Structures", *IEEE Trans. on Power Delivery*, Vol. 22, Issue 1, January 2007, pp.619-626.

[21] R. Benato, D. Napolitano, "Reliability Assessment of EHV Gas Insulated Transmission Lines: effect of redundancies", *IEEE Trans. on Power Delivery*, Vol. 23, Issue 4, October 2008, pp. 2174-2181.

[22] R. Benato, R. Caldon, A. Paolucci, "An automatic procedure for the computation of electromagnetic interferences in different power systems," *Proc. of 97a Riunione Annuale AEI*, Vol. 3, Baveno 1997, pp. 19-26 (in Italian).

[23] R. Benato, R. Caldon, A. Paolucci, "Matrix algorithm for the analysis of high speed railway and its supply system," *L'Energia Elettrica*, Vol. 75, N°. 5, September-October 1998, pp. 304-311 (in Italian).

[24] J. Arrillaga, C.P. Arnold, *Computer Analysis of power systems*, John Wiley & Sons, New York, 1990.

[25] CCITT: "Directives concerning the protection of telecommunication lines against harmful effects from electric power and electrified railway lines." Geneve, 1989.

[26] A. Hochrainer, *Symmetrische Komponenten in Drehstromsystemen* (Chap. 15), Springer, Berlin, 1957.

[27] R. Benato, "Multiconductor Analysis of Underground Power Transmission Systems: EHV AC Cables," *Electric Power Systems Research*, Vol. 79, Issue 1, January 2009, pp. 27-38, doi: :10.1016/j.epsr.2008.05.016.

[28] C. L. Fortescue, "Method of symmetrical co-ordinates applied to the solution of polyphase networks," in Proceedings of the A.I.E.E., vol. 37, Part II, pp. 1027-1140, June 1918.